13th International Symposium on Particle Image Velocimetry – ISPIV 2019
Munich, Germany, July 22-24, 2019

Evaluation of tumble ratio of an SI engine in steady flow bench by SPIV measurements

Giwon Yun[1], Jaeyong Sung[2]*, Inyong Ohm[2]

[1]SeoulTech / Graduate School / Seoul, Republic of Korea
[2]SeoulTech/ Department of Mechanical & Automotive Engineering / Seoul, Republic of Korea
*jysung@seoultech.ac.kr

Abstract

Tumble ratio, a quantitative index of the tumble flow, is a major factor in the performance evaluation of an SI engine. For the accurate evaluation of tumble ratio from velocity data, 3D velocity components in streamwise plane are necessary. Thus, in this paper, a stereoscopic PIV is applied to investigate the tumble flow in an SI engine. The experiments were conducted in the SI engine head for several fixed valve lifts and 383mmH2O pressure difference across the intake valves. Tumble flow analysis was carried out in a plane perpendicular to the cylinder axis located at 0.5S(49.5mm) below the engine head. The results show the flow coefficient increases rapidly when the valve lift increases from 1mm to 4mm. Then, at the valve lift more than 4mm, the flow coefficient maintains a nearly constant value. In addition, the tumble coefficient increases substantially when the valve lift increases. Exceptionally, the tumble coefficient has a local maximum when the valve lift is 1mm and 9mm. This is caused by the change of flow structure in the cylinder according to the valve lift. Finally, the mean flow coefficient and the tumble ratio of the SI engine used in this study are evaluated as 0.203 and 3.557, respectively.

1 Introduction

During the four-stroke cycle of an SI engine, the flow characteristics at the end of the compression stroke govern the mixing of fuel and air, which affects the in-cylinder combustion. There are two kinds of vortex flow formed in a short time of the end of compression stroke. One is swirl flow and the other is tumble flow. Although both the flows are important in the engine performance, the present study focused on the tumble flow, which is vertically rotating flow along the axis of engine cylinder. Tumble ratio, a quantitative index of the tumble flow, is a major factor in the performance evaluation of an SI engine.

Prior to a real engine test, a test bench of cold and steady flow is fulfilled for the evaluation of the flow characteristics. To measure the tumble flow in the steady flow bench, several methods have been applied, such as LDV (laser Doppler velocimetry) (Kang & Baek (1995), Liu & Santavicca (1985), Le Coz et al. (1990)), 2D PIV (particle image velocimetry) (Alger et al. (2003), Kim et al. (2006)) and ISM (impulse swirl meter) combined with a T-pipe method (El-Adawy et al. (2018)). In the ISM measurement, it is difficult to evaluate the accurate tumble ratio due to the reduction of the torque when the flow passing through the T-pipe. LDV and 2D PIV have also disadvantage in sense that these techniques do not give 3D velocity components inside the whole area. For the accurate evaluation of tumble ratio from velocity data, 3D velocity components in streamwise plane are necessary. Recently, 3D-tumble flow using stereoscopic PIV is being studied on the vertical plane of the cylinder (Calendini et al. (2000), Park & Ohm (2015)). However, there is little research on the evaluation of tumble flow of SI engine using stereoscopic PIV.

Thus, in this paper, a stereoscopic PIV is applied to investigate the tumble flow on the measurement plane perpendicular to the cylinder axis in an SI engine. The mean flow coefficient and tumble ratio,

which are the performance indicators of the SI engine, are evaluated. In addition, the effects of valve lift on the 3D velocity, flow coefficient and tumble coefficient are discussed.

2 Experimental Setup

Figure 1 shows the schematic of the experimental setup of the stereoscopic PIV in the steady state flow experiment. The main components of the device can be divided into two parts: First, the experimental setup of stereoscopic PIV consisted of two CCD cameras (Power view Plus 4MP), two tilt lenses (PC micro f/2.8D), two camera bases, pulsed laser system, laser mirror, three-axis conveying device and analysis software for data processing (INSIGHT 4G, TSI). Second, the main components of the steady flow device are valve lift controller, blower, inverter and pressure gauge. In this experiment, a flow box based on a four-valve SI engine is used. Table 1 shows the specifications of the SI engine used in the experiment.

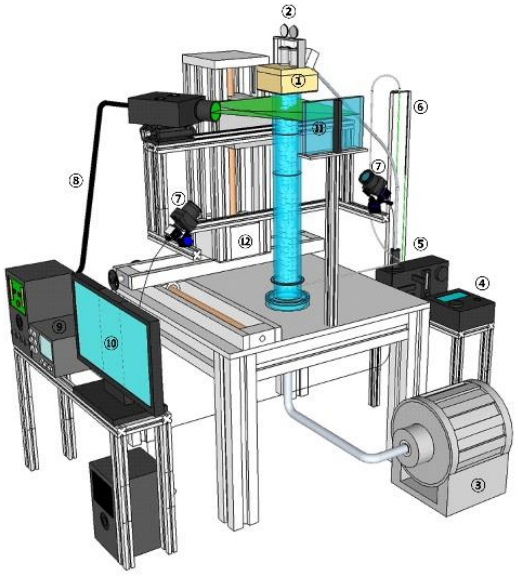

1. Engine head flow box, 2. Valve lift controller, 3. blower, 4. Inverter, 5. Particle generator, 6. Pressure gauge, 7. CCD camera, 8. ND-YAG Laser, 9. Synchronizer, 10. Data acquisition system, 11. Laser mirror, 12. Camera translation system

Figure 1: The schematic of experimental setup of the stereoscopic PIV in the steady state flow experiment

Figure 2(a) shows the measurement position and coordinate axes. The measurement position is 0.5S (49.5mm) below the engine head and the velocity filed in the plane perpendicular to the cylinder axis is measured while adjusting the valve lift 1mm to 10mm with an 1 mm increment. In this case, the pressure difference across the intake valve is performed at a constant value of 383 mmH2O. The cylinder used in the experiment was made of transparent acrylic to observe the flow inside the cylinder. It is located between the two cameras, limiting the vertical positioning of the measurement plane and the optical axis of the camera. In this experiment, the optical axis of the camera was positioned at a constant angle to the measured plane. Distortion is caused by the cylinder wall. This distortion was corrected using a three-dimensional calibration test presented by Soloff et al. (1997). A 2-layer target was used for calibration experiment. Figure 2(b) shows the scheimpflug stereoscopic cameras and laser mirror configuration. The scheimpflug principle was fulfilled when the best focus

over the entire image, for each camera, was achieved using a tilt lens and 3-axis rotating camera bases. Also, the laser path was extended using a laser mirror so that laser width is larger than the cylinder diameter and the laser thickness is 2mm in the measurement position. The illuminated particles were recorded with a pair of CCD cameras. For every valve lift, 300 pairs of images were acquired. The commercial software INSIGHT 4G was used for processing of the acquired images to obtain the velocity vector fields. Adaptive recursive correlation techniques with a size of 32 × 32 pixels interrogation area was implemented. A specification of steady-state flow bench and stereoscopic PIV is included in table 2.

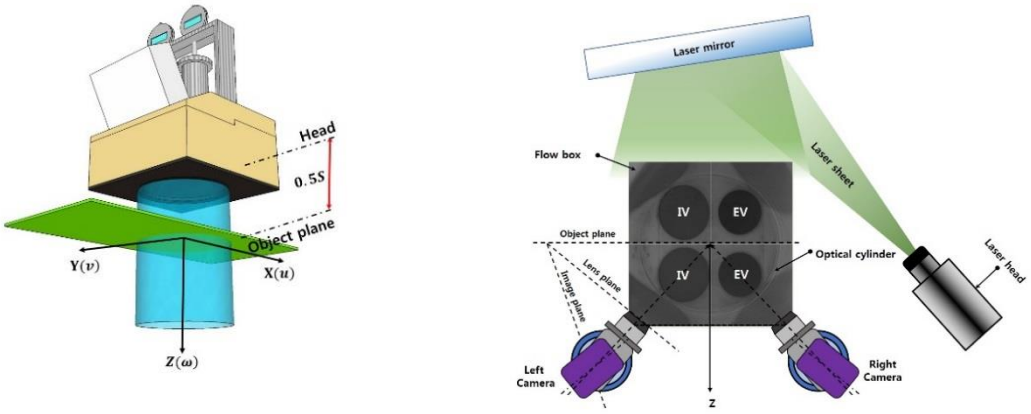

(a) (b)

Figure 2: (a) The measurement position and coordinate axes and (b) The scheimpflug stereoscopic cameras and laser mirror configuration

Table 1: SI engine specifications

SI engine specifications	
Intake port design	Tumble port
Displacement	1.6L
Bore diameter [B]	75.6mm
Stroke length [S]	89mm

Table 2: Specifications of steady-state flow bench and stereoscopic PIV

Specifications of stereoscopic PIV		
Valve lift		1~10mm, 1mm increment
Measuring position		0.5S (49.5 mm from Head)
Pressure drop		15"H_2O(383mmH_2O)
Laser Pulse	Separation (Δt) Frequency Width	10μs 1Hz 2mm
Sampling Raw Data NO.		300
Processing	Calibration Interrogation Reconstruction method	2-layer target 32pixel × 32pixel Three-dimensional calibration
Particle	Type Size No.density Stokes NO.	Olive oil < 1 μm 10^7 particles/cm^3 <<1

3 Results and Discussion

3 .1 Effect of valve lift on flow coefficient and tumble coefficient

The mean velocity field was obtained by averaging 300 velocity fields for each valve lift. Figure 3 shows measurement plane and the vector and velocity contours of the mean velocity fields for the valve lift of 10mm. Figure 3 (a) show the measurement plane. The + x-axis area is just below the intake valve and the – x-axis area is just below the exhaust valve. Figure 3 (b), (c) and (d) show the velocity distribution of U ,V and W , respectively. The velocity components at each coordinate are used to calculate the flow coefficient and tumble coefficient (Xu (2001), Oosthuizen & Carscallen (1997), White (2011)).

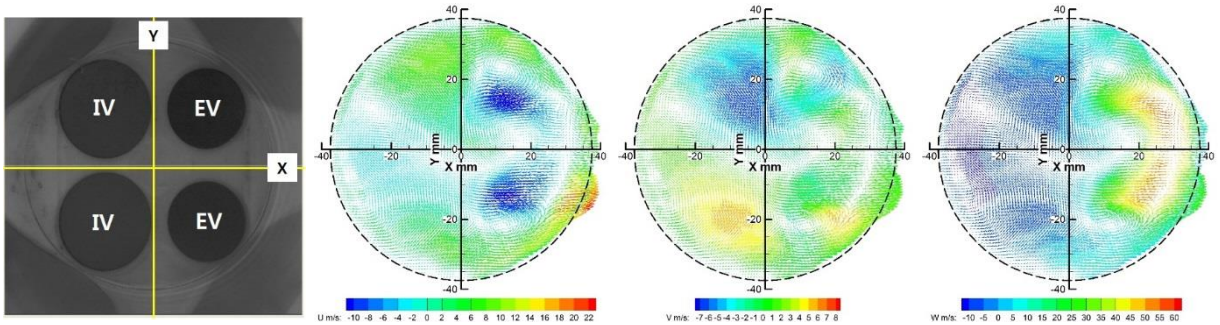

(a) measurement plane (b) U - velocity (c) V – velocity (d) W - velocity

Figure 3: Measurement plane and 3D velocity components at valve lift = 10mm

The flow coefficient is the real mass flow rate non-dimensionalized by the theoretical mass flow that can flow through the valve inner seat area rather than the real air flow area. Therefore, the flow coefficient is defined as

$$C_f = \frac{\dot{m}_{real}}{\dot{m}_{theory}} = \frac{4\dot{m}}{\rho v_0 \pi D^2} \tag{1}$$

where $\dot{m}$: the real mass flow rate measured by stereoscopic PIV [kg/s], ρ : the density of adiabatic air[kg/m^3], v_0 : the theorical velocity[m/s], D : inner seat diameter[mm]. In a steady-state flow test, it is assumed that the flow is adiabatic. Therefore, the theoretical velocity v_0 is calculated as

$$v_0 = [2C_p(T_0 - T)]^{1/2} = \left[\frac{2\gamma}{\gamma - 1} RT_0 \left(1 - (P/P_0)^{\frac{\gamma}{1-\gamma}}\right)\right]^{1/2} \tag{2}$$

where γ : specific heat ratio of the air, R : gas constant[$J/kg \cdot K$], T_0 : Normal temperature[K], P_0 : Normal pressure[Pa], P : Pressure in the cylinder[Pa].
The tumble coefficient (N_t) is the ratio of the angular momentum to the momentum of intake flow. Therefore, the tumble coefficient (N_t) is defined as

$$N_t = \frac{\text{tumble momentum}}{\text{intake momentum}} = \frac{\omega_t \cdot B \cdot \dot{m}}{v_0 \cdot \dot{m}} = \frac{8T}{\dot{m} \cdot v_0 \cdot B} \tag{3}$$

where T : tumble momentum calculated by stereoscopic PIV[$N \cdot m$], $\dot{m}$: the real mass flow rate[kg/s], v_0 : the theorical velocity[m/s], B : cylinder bore size[mm]

In steady state flow, the tumble momentum is defined by the angular momentum equation. Also, the tumble momentum is calculated by using the velocity and area component obtained from the stereoscopic PIV.

$$T = \int (r \times V) \rho V \cdot dA = \int \rho x v_z v_z dA \tag{4}$$

Figure 4 shows the three-dimensional vector field measured by stereoscopic PIV in the perpendicular plane to the cylinder axis at various valve lifts. Absolute velocity is calculated by using U ,V and W velocity components as follows;

$$v_{abs} = \sqrt{\left(v_x^{\,2} + v_y^{\,2} + v_z^{\,2}\right)} \tag{5}$$

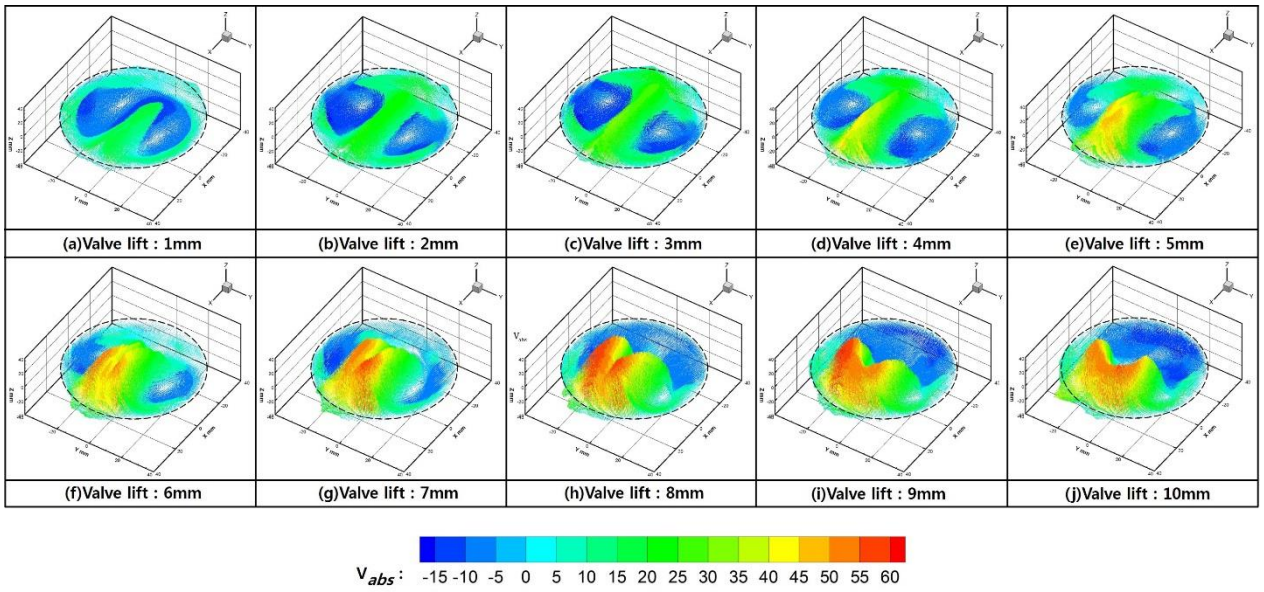

Figure 4: 3D-vector and contour of absolute velocity at various valve lifts

Figure 4(a) shows the absolute velocity field at valve lifts 1mm. At this valve lift, a weak tumble flow in the counterclockwise direction is generated. The incoming air into the cylinder forms downward flow along the cylinder center(y=0) from the intake valve toward the exhaust valve. Also, an upward flow between the intake valve and the exhaust valve is symmetrically formed to cylinder center (y=0). Figure 4(b)-(C) show the absolute velocity 3D-vector field at valve lifts 2mm,3mm, respectively. With increasing the valve lift from 2mm to 3mm, the more air flows toward the exhaust side by the intake port. Unlike the 1mm valve lift, a larger downward flow is formed at the intake valve region. Also, the upward flow is formed only between the intake valve and the exhaust valve. Figure 4(d)-(i) show the absolute velocity 3D-vector field at valve lifts from 4mm to 9mm, respectively. With increasing the valve lift from 4mm to 9mm, the more air flows toward the exhaust side by the intake port, then downward flow is gradually deflected toward the exhaust valve region. In addition, upward flow is gradually deflected toward the intake valve region. The velocity of the deflection flow becomes larger with increasing the valve lift, the tumble flow is formed strongly in counterclockwise direction. Figure4(j) show the absolute velocity 3D-vector field at valve lift 10mm. Compared with valve lift

9mm, the maximum velocity is reduced but the downward flow region in the exhaust valve is formed wider.

Figure 5 shows the tumble momentum distribution with various valve lift. Figure 5(a) shows the tumble momentum at valve lift 1mm. At this valve lift, a relatively large momentum formed near exhaust valve region. Figure 5(b)-(c) shows distribution of the momentum at valve lift of 2mm and 3mm, respectively. At these valve lifts, tumble momentum in the exhaust valve gradually increases with the valve lift. In addition, in the intake valve, the momentum gradually increases with increasing the valve lift in the opposite direction of the exhaust valve. This momentum distribution is due to the increase in the descending flow at the intake valve and the exhaust valve, as shown in fig. 4(b)-(c). Figure 5(d)-(e) shows distribution of the tumble momentum at valve lift of 4mm and 5mm, respectively. With increasing the valve lift from 4mm to 5mm, momentum in the exhaust valve gradually increases. However, in the intake vale, the momentum gradually decreases with the valve lift. Momentum reduction in the intake valve is due to increase the upward flow toward the intake valve with increasing the valve lift as shown in fig. 4(d)-(e). Figure 5(f)-(j) shows distribution of the tumble momentum at valve lift from 6mm to 10mm, respectively. With increasing the valve lift from 6mm to 10mm, momentum in the exhaust valve gradually increases. In addition, the area of strong momentum gradually becomes closer and wider to the cylinder wall at the exhaust valve side. Momentum increase in the exhaust valve results from that downward flow becomes stronger with increasing the valve lift as shown in fig. 4(f)-(j).

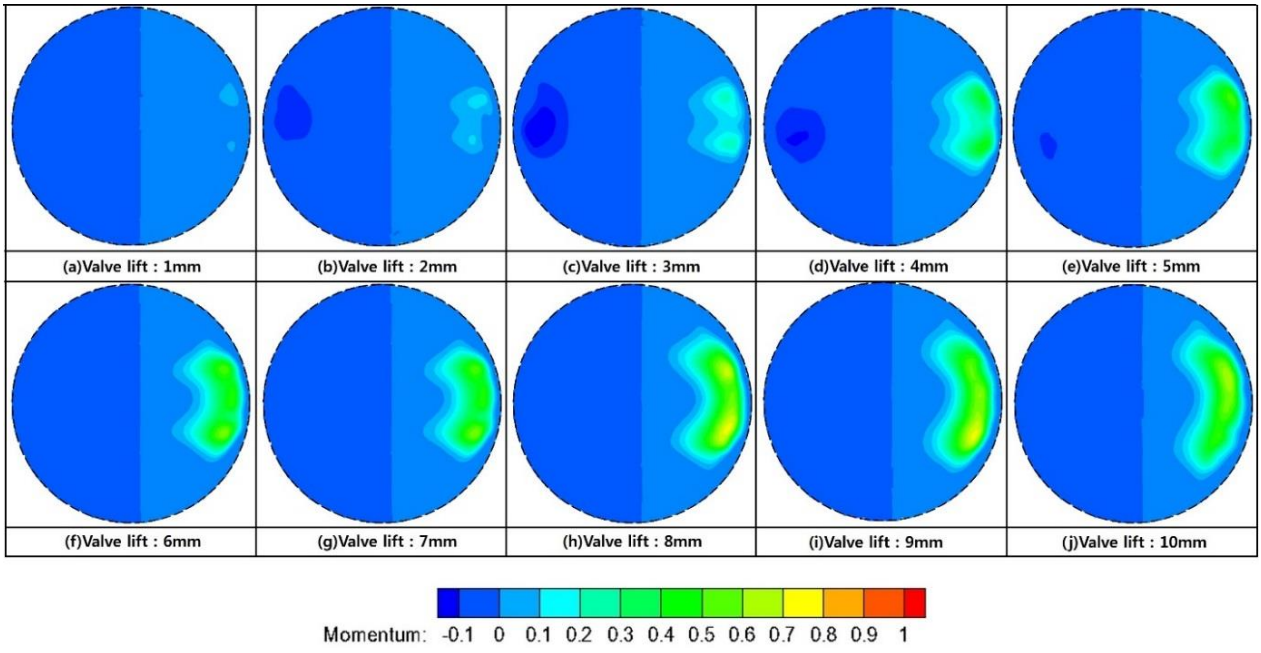

Figure 5: Tumble momentum at various valve lifts

Figure 6 show the variation of the flow coefficient (C_f) and the tumble coefficient (N_t) with valve lifts. These results represent that variation of the flow structure due to the change of valve lift affects C_f and N_t. Figure 6(a) represents the variation of the flow coefficient (C_f). It is observed that C_f increases rapidly for 1 to 4 mm valve lift. In particular, C_f increases most steeply when the valve lift changes from 1mm to 2mm. After 4mm valve lift, C_f maintains a nearly constant value (Within 5% of average value of 0.2738 between the valve lift 4mm and 10mm). After the valve lift of 4mm, the tumble flow becomes stronger as shown in fig. 4, so that a downward flow is formed on the exhaust valve and an upward flow is formed on the intake valve. By this flow structure, the actual mass flow

rate passing through the measurement plane is similar and C_f seems to be constant regardless of the valve lift. Figure 6(b) shows the variation of the tumble coefficient (N_t) according to the valve lift. It is shown that N_t decreases for 1-2mm valve lift. When the valve lift is 2-3mm, N_t increases slightly. Then, it starts to increase rapidly with increasing valve lift from 4mm to 9mm. On the contrary, at 10mm valve lift, N_t decreases. At the valve lift of 1mm, a downward flow and an upward flow are formed in the exhaust valve and intake valve, respectively, and a tumble flow is generated. However, at the valve lift 2mm and 3mm, a downward flow is formed not only at the exhaust valve side but also at the intake valve side as shown in fig. 4. In addition, the momentum in the opposite direction is generated at the intake and exhaust valve sides as shown in fig. 5. As a result, at the valve lift of 2-3mm, the ratio of momentum sum over the real mass flow rate decreases compared with 1mm valve lift, so that N_t is decreased. Even though the valve lift is 4mm and 5mm, the momentum in the opposite direction at the intake-exhaust valve formed, but the momentum at the exhaust valve is large and N_t increases compared to the case of the valve lift 1mm. At the valve lift of 10mm, the momentum is similar but the real mass flow rate increases as compared to valve lift of 9mm. Therefore, the ratio of momentum sum over the real mass flow rate decreases compared with 9mm valve lift, so that N_t is decreased.

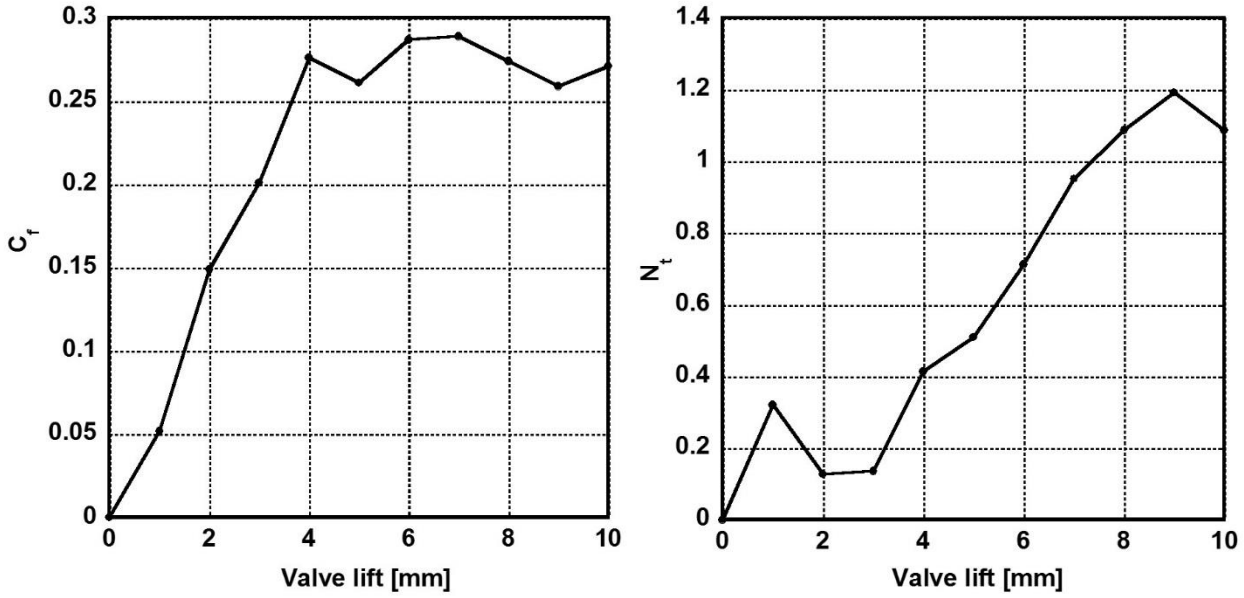

(a)Flow coefficient (C_f) (b) Tumble coefficient (N_t)

Figure 6: Variation of the flow coefficient and the tumble coefficient according to the valve lift

3 .2 Mean flow coefficient (C_{f_mean}) and Tumble ratio (R_t)

Mean flow coefficient (C_{f_mean}) is a normalized parameter for the assessment of overall port efficiency. In this study, C_{f_mean} is defined by considering the intake process to start at IVO (intake valve open) and end at IVC (intake valve close) [11-13]. Therefore, C_{f_mean} is defined as

$$C_{f\_mean} = \frac{\int_{\alpha_1}^{\alpha_2} C_f \, d\alpha}{\alpha_2 - \alpha_1} \tag{5}$$

where, C_f : flow coefficient, α_1 , α_2 : inlet valve open and close position crank angle respectively.

In steady-state flow test, the vortex rotation speed is commonly calculated assuming that the charge motion is a solid body rotating flow which, at the end of induction process, has a momentum equal to the sum of the angular momentum introduced during the whole induction process. The tumble ratio (R_t)is calculated by integrating N_t as a function of crank angle during the induction process and then divided by the fictitious engine speed. [11-13] Therefore, R_t is defined as,

$$R_t = \frac{BS}{n_v D_{ISD}^{\ 2}} \cdot \frac{\int_{\alpha_1}^{\alpha_2} C_f \cdot N_t \, d\alpha}{\left(\int_{\alpha_1}^{\alpha_2} C_f \, d\alpha \right)^2} \tag{6}$$

where, B : cylinder bore[mm], S : engine stroke[mm], n_v : number of valve, D_{ISD} : inner seat diameter[mm], C_f : flow coefficient, α_1 , α_2 : inlet valve open and close positions of crank angle respectively, N_t : tumble coefficient. To obtain C_{f_mean} , R_t and α in each valve lift should be defined. α is defined by a normalized valve angle for each valve lift through standard valve pressure curve. The calculation of the crank angle is omitted. The mean flow coefficient and tumble ratio of the present SI engine are evaluated as shown in Table 3.

Table 3: SI engine of mean flow coefficient and tumble ratio

The mean flow coefficient and tumble ratio of the present SI engine	
Mean flow coefficient (C_{f_mean})	0.203
Tumble ratio (R_t **)**	3.557

4 Conclusions

In this study, the effect of valve lift on the flow coefficient and the tumble coefficient has been investigated experimentally using a stereoscopic PIV. The mean flow coefficient and the tumble ratio of the SI engine used in this study are evaluated as 0.203 and 3.557, respectively. The following conclusions were drawn.

1. Through the 3D velocity vector field obtained by the stereoscopic PIV measurement, it was founded that as the valve lift increases from 1mm to 2mm, the tumble flow decreases. In addition, for the valve lift more than 2mm, the downward flow becomes stronger at the exhaust valve region and the upward flow becomes stronger at the intake valve region.

2. With increasing the valve lift, the momentum strength at the exhaust valve region increases substantially and the momentum in the opposite direction that is formed in the intake valve region decreases.

3. The strong momentum at the exhaust valve region is formed closer to cylinder wall and is distributed wider as the valve lift increases.

4. The flow coefficient increases rapidly when the valve lift increases from 1mm to 4mm. Then, at the valve lift more than 4mm, the flow coefficient maintains a nearly constant value.

5. The tumble coefficient increases substantially when the valve lift increases. Exceptionally, the tumble coefficient has a local maximum when the valve lift is 1mm and 9mm. This is caused by the change of flow structure in the cylinder according to the valve lift.

Acknowledgements

This research was supported by Daeyun MS Co Ltd.

References

Alger T, Blobaum E, McGee J, Wooldridge S (2003) PIV characterization of a 4-valve engine with a camshaft profile switching (CPS) system. *SAE Transactions J. Fuels & Lubricants* 112:1066-1078

Calendini PO, Duverger T, Lecerf A, Trinite M (2000) In-cylinder velocity measurements with stereoscopic particle image velocimetry in a SI engine. *J. Fuels & Lubricants* 109:951-961

El-Adawy M, Heikal MR, Aziz ARA (2018) Stereoscopic particle image velocimetry measurements and proper orthogonal decomposition analysis of the in-cylinder flow of gasoline direct injection engine. *J. Energy Resources Technology* 141: doi: 10.1115/1.4042068

Kang KY, Baek JH (1995) LDV measurement and analysis of tumble formation and decay in a four-valve engine. *Experimental Thermal and Fluid Science* 11:181-189

Kim M, Lee S, Kim W (2006) Tumble flow measurements using three different methods and its effects on fuel economy and emissions. *SAE Technical Paper* 2006-01-3345

Le Coz JF, Henriot S, Pinchon P (1990) An experimental and computational analysis of the flow field in a four-valve spark engine-focus on cycle-resolved turbulence. *SAE Transactions J. Engines* 99:294-321

Liu TM, Santavicca DA (1985) Cycle resolved LDV measurements in motored IC engine. *J. Fluid Engineering* 107:232-240

Park C, Ohm I (2015) Study on evaluation method of flow characteristics in steady flow bench (1) – raising issue. *Transactions of KSAE* 23: 88-96

Oosthuizen PH, Carscallen WE (1997) *Introduction to Compressible Fluid Flow*. One-Dimensional Isentropic Flow, page 54-57. McGraw-Hill. 1997 edition

Soloff SM, Adrian RJ, Liu ZC (1997) Distortion compensation for generalized stereoscopic particle image velocimetry. *Measurement Science and Technology* 8:1441-1454

White FM (2011) *Fluid Mechanics*. Integral Relations for a Control Volume, page 186-187. McGraw-Hill. 7th edition

Xu, H (2001) Some critical technical issues on the steady flow testing of cylinder heads. *SAE Technical Paper* 2001-01-1308